An Automated System of Soil Sensor-based Site-specific Seeding for Silage Maize: A Proof of Concept

Muhammad Abdul Munnaf[1], Abdul Mounem Mouazen[1,*]
[1]Department of Environment, Ghent University, Coupure Links 653, 9000 Gent, Belgium
[*]E-mail of the corresponding author: abdul.mouazen@ugent.be

Abstract

Despite recent studies of map-based site-specific seeding (SSS) revealing improved agronomic and economic outcomes over uniform rate seeding (URS), to our best knowledge no visible and near infrared spectroscopy (vis-NIRS) sensor-based SSS studies exist to date. This study aimed to develop and evaluate an automated sensor-based SSS technology for silage maize (*Zea mays* L.) production. An on-line visible and near-infrared reflectance spectroscopy (vis-NIRS) sensor was installed in front of a tractor to provide real-time input data to control the seed rate using a precision seeding machine mounted at the back of the tractor. A LabVIEW-based software was developed and used to predict soil fertility index using on-line vis-NIR spectra, which was then used to calculate the seed rate and transfer it to the controller of the seeding machine. The agronomic and economic benefits of SSS were compared with URS for silage maize production under a one-site-year experiment. Results showed that the proposed sensor-based SSS technology was 87.5% efficient in controlling the desired seed rates, according to the soil fertility status. In parallel with the observed spatial similarity between predicted soil fertility index and actual seed rates, a strong linear association (R^2=0.80) was also achieved. As a result, SSS improved silage yield by 1.4 t ha^{-1} (4.4%), while sowing a lower seed rate (86.4 kSeeds ha^{-1}) than the URS (90 kSeeds ha^{-1}). This improved gross margin by 91 € ha^{-1}, of which only 7 € ha^{-1} was attributed to savings on seed cost. The proposed sensor-based SSS technology was technically sound and thus transform within-field fertility variations into agro-economic benefits effectively.

Keywords: Automation; Precision agriculture; Soil sensing; Decision support system; Soil fertility assessment; Yield and Cost-benefit analysis

1 Introduction

Site-specific seeding (SSS) is a precision farming operation aiming to manage in-field soil variations by optimizing seeding rates as per fertility and yield potential of different parts of a field (Isbell, 2005). The SSS concept has been developed to solve issues related to the traditional uniform rate seeding (URS) approach that uses a uniform seed rate throughout a field. By the URS in-field fertility spatial variations are overlooked, hence, sub-optimal plant populations are grown at different parts of a field. In densely planted zones inter-crop competition for nutrients, sunlight, and water rise, whereas in sparsely seeded zones weeds grow more intensively, hence, optimal crop growth and yield are negatively affected (Jiang et al., 2013). Therefore, the overall yield harvested is below the yield potential of a field, which reduces the production margin.

The SSS is implemented as map-based and sensor-based methods (Munnaf et al., 2021). The map-based SSS concerns the adjustment of the application rate according to the previously developed application map. The most positive aspect of a map-based system is that it allows sufficient time between sensing and application, which is useful to facilitate proper data processing for improving overall application accuracy. Recommendations are made at the office in consultation with farmers, agronomists, and experts. Predefined recommendations allow for a “look ahead” system, which improves controller responses and smoothens the SSS in transition. In this principle, point locations on the application map and corresponding field points should be well synchronized by a proper geo-referencing system (Grisso et al., 2011). Munnaf et al. (2022) and Munnaf & Mouazen (2021b) implemented map-based SSS evaluated for seed potato, consumable potato and grain maize using in advance developed management zone maps delineated by fusion of soil fertility and crop information. By adopting the “Kings” approach that recommended the highest seeding rate for the most fertile zone and vice versa, authors reported increases crop yields (1.0 to 4.8 t ha^{-1} for potato; and 0.70 t ha^{-1} for maize) as well as gross margin (380 to 597 € ha^{-1} for potato; and 93 € ha^{-1} for grain maize). Using soil apparent electrical conductivity to map soil fertility variation, Kempenaar et al. (2017) reported that map-based SSS could increase potato yield by 4% compared to the URS. Conversely, the point synchronization feature makes this system highly sensitive to an error associated with the miss placement of seeds. Map-based systems are not suitable for sudden change in soil conditions attributed to weather circumstances e.g., rainfall and drought, which may occur between mapping variability and implementing SSS. Therefore, a system that can overcome the limitations of the map-based approach is necessary to be developed.

The concept of sensor-based SSS system can overcome the limitations of the map-based approach. In the sensor-based SSS, high-resolution data collected with advanced sensor technologies are needed in real-time. This continuous stream of sensor data is transferred and converted successively into information and recommendations to be implemented by a proper controller, all applied in real-time (Grisso et al., 2011). It does not require a differential global positioning system (DGPS) and application map, and thus it is free from error regarding locations of sampling points, the position of the applicator, and map interpolation issues. Unlike map-based application, it is free from the issue regarding sudden change in soil conditions due to weather circumstances.

Apart from the application method, another important aspect in successful implementation of SSS is to assess in-field yield potential accurately and rapidly, which is crucial for sensor-based application. Deciding seed rates depending on a single soil proxy information that never reflects yield potential effectively while a fusion of multiple soil information can represent soil fertility more accurately and thus true yield potential of a field. Assessing soil fertility using a soil fertility index (SFI) is well documented (Andrews et al., 2004). A SFI is a mathematical combination of several soil fertility attributes weighted by some loading factors. Such an SFI has recently been developed and validated to accurately predict and map spatial variation in soil fertility using an on-line visible and near infrared spectroscopy (vis-NIRS) soil sensor (Munnaf & Mouazen, 2021). It is hypothesized that this SFI is an accurate parameter indicating the actual spatial variation in soil fertility, hence, it can be used for successful implementation of sensor-based SSS.

Several sensor-based site-specific applications have already been developed and evaluated for variable-rate fertilizer application (Chattha et al., 2014; Maleki et al., 2008; Maleki and Zamiran, 2009; Mouazen and Kuang, 2016), and spot applications for agrochemicals and fungicide (Esau et al., 2014a, 2014b). Maleki et al. (2008) attached an on-line vis-NIRS soil sensor (Mouazen, 2006) in front of a maize (*Zea mays* L.) planter to measure soil available phosphorous (P) and accordingly calculate and apply P_2O_5 at variable rate according to P value measured. Chattha et al., (2014) proposed an on-the-go system of variable-rate fertilization using a nozzle control mechanism where they identified bare spots in the blueberry field using µ-eye colour cameras mounted in front of the tractor. Later, a similar technology was evaluated for herbicide and fungicide application for wild blueberry production (Esau et al., 2014b, 2014a). A sensor-based variable rate nitrogen (N) fertilization system is commercially available, which uses a multispectral sensor to measure crop N content to be used as input to a spinning disc fertilizer spreader to adjust the N application rate behind the tractor in real-time (Guerrero et al., 2021). However, no study has been found in the literature about the sensor-based SSS application to date.

Therefore, this study aims to develop and evaluate a fully automated sensor-based SSS technology. The novelty of this study goes beyond the state-of-the-art through real-time soil fertility assessment by the on-line vis-NIRS sensor (Mouazen, 2006), and developing a decision support system for calculating and controlling seed rates in real-time. Finally, this study evaluated the agronomic and economic performance of the proposed technology in silage maize.

2 Materials and methods

2.1 Sensor and planter development

The on-line vis-NIRS sensing platform previously developed and patented by Mouazen (2006) was adopted after modifications to allow mounting it at the front of the tractor instead of the back of the tractor. The sensor platform consists of a subsoiler that makes 15 to 20 cm deep trenches in the topsoil, the bottom of which is smoothened by the subsoiler itself due to its downward forces. An optical probe hosted in a mild steel holder (appended at the backside of the subsoiler chisel) measures soil spectra in diffuse reflectance mode from the smoothed bottom of the trench. A fibre-type spectrophotometer (CompactSpec from Tec5 Technology, Germany), with a spectral range of 305 to 1700 nm and a sampling resolution of 1 nm was used to record soil spectra at a frequency of 1 Hz. A ≃ 99% PTFE (Polytetrafluoroethylene) disc of 60 mm in diameter was used as the white reference to recalibrate the sensor once every 30 min.

A 3 m wide (4x75 cm) fully mounted type precision seeding machine (Kverneland Optima Rigid e-Drive, The Netherlands) was attached to the three-point hitch at the back of the tractor. The tractor was equipped with a GNSS (Global Navigation Satellite System) receiver (NAV-900, Trimble, USA) to provide a high-precision auto-guidance. This planter machine is equipped with optical seed counters, which are controlled individually via electric motor by the task controller attached to the seeding machine. The task controller receives input from the virtual terminal in the tractor cabin using an ISObus communication protocol. A virtual terminal named IsoMatch Tellus PRO (Kverneland group, The Netherlands) was used in this work. It has three options for assigning seed rates: 1) manual input through the touch screen of the virtual terminal, 2) uploading seed rates map as ISOxml task card, and 3) sending seed rates from an external device through the serial communication. This study used the third option to control seed rate by sending a command message from a custom-made decision processor. Figure 1 shows the proposed sensor-based SSS system. Its geo-control functionality automatically switches a seeding unit on or off in exactly the right place, ensuring no overlap with any row that has already been sown.

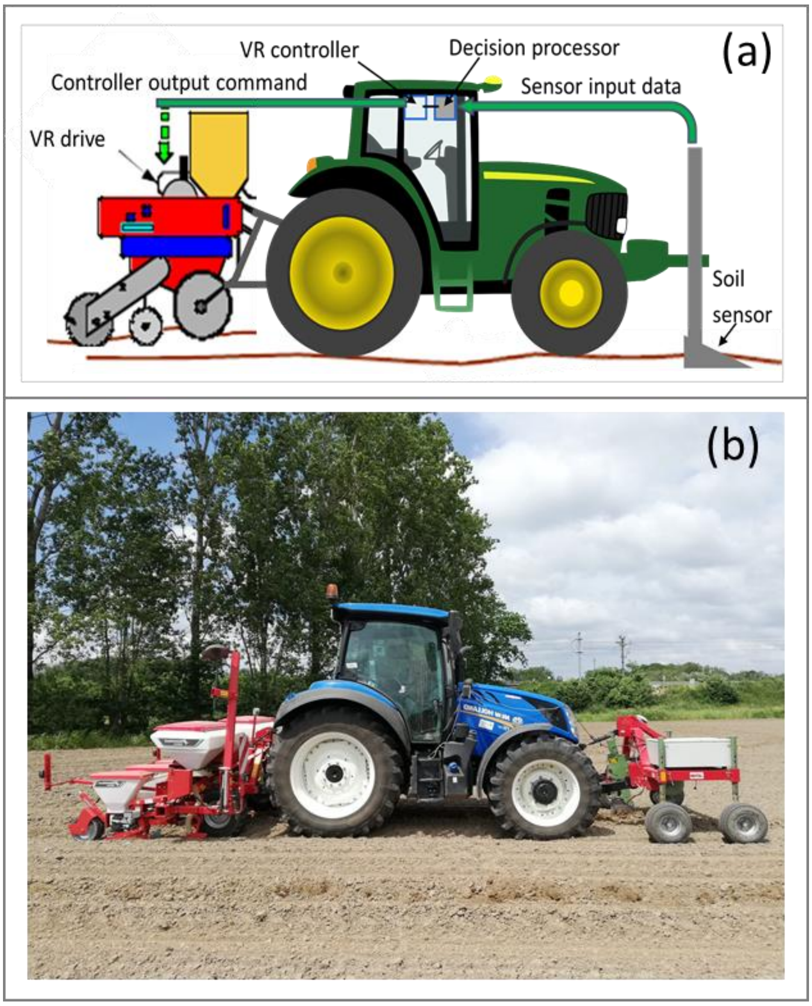

Figure 1 An illustration of sensor-based site-specific seeding system shown as (a) sketch and (b) in real field application. VR, variable rate.

2.2 Software development

A decision processing software was developed using LabVIEW (Laboratory Virtual Instrumentation Engineering Workbench) programming language (National Instrument Inc., USA, version 10.0f1) to enable real-time soil sensing, SFI prediction, seed rate calculation, and communication with the virtual terminal. This software package was then installed on a semi-ruggedized laptop computer (Toughbook, Panasonic UK Ltd., Bracknell, UK). It has three modules i.e., soil fertility assessment, seed rate decision, and task control. While the tractor moves forward, the fertility assessment module records soil spectra, pre-processes them by averaging 5 successive spectra into one spectrum, edge trimming to 400-1690 nm, moving average and min-max normalization. A previously developed partial least squares regression (PLSR) model, similar to the one reported in our previous study (Munnaf & Mouazen, 2021), was used to predict the on-line SFI once per 5 seconds (the equivalent of 6.9 m of tractor travel distance). Since the SFI range was narrow (1 to 4.52) for this field (Munnaf & Mouazen, 2021), the SFI was rescaled to a range of 0 to 10. The seed rate decision module starts with filtering out values outside the $0 \leq SFI \leq 10$ range, followed by assigning the URS seed rate of 90 kSeeds ha^{-1} (in other words 90000 seeds ha^{-1}) or continues the previous seed rate until a different value is calculated and sent as the next seed rate command. The 0 to 10 SFI range is divided into five classes, to which five different seed rates were assigned accordingly, as shown in Figure 2. Seed rate was calculated following the Kings principles i.e., sowing most densely in the highest SFI class (Munnaf & Mouazen, 2021). The task control module generates an NMEA (National Marine Electronics Association) message containing seed rate information as a string packet and transfers it to the virtual terminal (IsoMatch Tellus PRO, Kverneland Group, The Netherlands) through the RS 232 port. The Tellus PRO then transfers seed rate messages to the task controller through the ISObus protocol and thus it controls seed rates. A response signal of actual seed rates sown in the ground was also received through the Rx channel of the RS 232 port. This serial communication was continuously sending and receiving seed rates information to and from the virtual terminal.

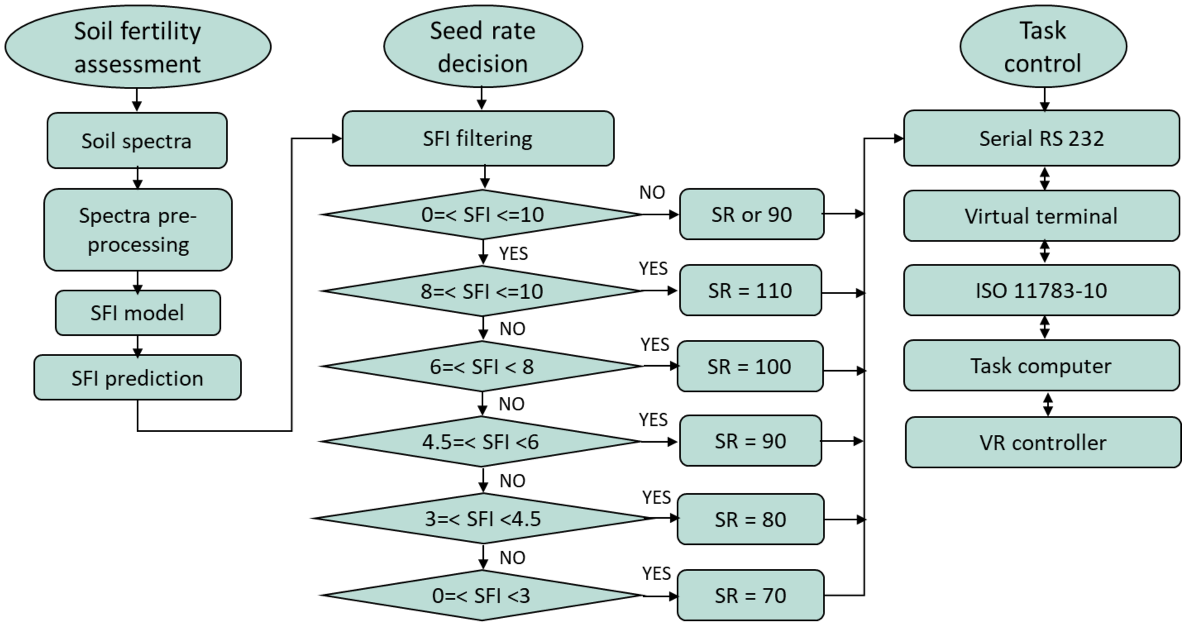

Figure 2 Block diagram of decision processing software developed for sensor-based site-specific seeding system. SR, seed rate; VR, variable rate; SFI, soil fertility index.

2.3 Time-distance lapse adjustment

Sowing seeds on the right point of that where SFI is measured is the key to succeed in a sensor-based application scheme. In this study, the on-line vis-NIRS sensor scanned one spectrum per second, while the seed rate was calculated per five seconds, which necessitate averaging five successive spectra into one spectrum to predict one SFI value. The same seed rate command was sent to the VR controller five times in the next five seconds, meaning that one seed rate per second was sent to the task controller, and the seed rate was updated once every five seconds. During these five seconds, tractor with a driving speed of 5 km hr^{-1} moves around 6.9 m, which is equal to the distance between the on-line soil sensor in front of the tractor and the seeding point at the back of the tractor (Figure 1). To adjust this initial distance gap, the first seed rate command was sent after five seconds of starting the system (Figure 3). Note that such a time-lapse adjustment necessitates a constant driving speed, and constant driving speed is not an issue of the modern tractors, which are equipped with an advanced navigation system like the one used in this study.

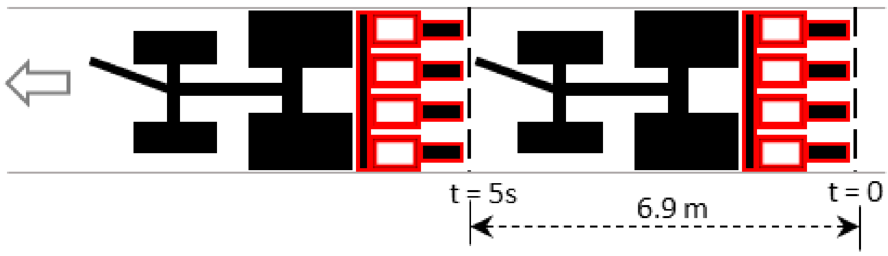

Figure 3 A schematic diagram of time-distance lapse adjustment.

2.4 Calibration of seeding system at the test plot

The proposed system was evaluated at first in a test plot of size 15 m x 100 m located next to the Bottelare farm in Ghent University, Belgium (50°57'45.6"N, 3°45'41.1"E). The soil was prepared as it should be prepared for actual seeding using a combination of rotavator, spike and drum harrows. Planter depth was set at 2.5 cm seeding depth by adjusting the downforce of each seeding unit. The seed hopper was full of sterile maize seed (unable to germinate) before starting the planting. A marker point was set at the starting and the ending point of the test plot. After calibrating the on-line vis-NIRS sensor using PTFE (Polytetrafluoroethylene) disc, the system applied different seeding rates throughout the 100 m plot length, while the tractor was driven at a driving speed of 3.5 km hr^{-1} . This low speed set in seeding system calibration was due to the use of a small tractor with short sensing-to-sowing distance i.e., ≈ 5 m. Five in-row sections of 2 m length (one per seed rate) were selected where the number of seeds was counted and recorded (Figure 4). The seeding densities were then calculated and compared with the defined seed rates (60, 80, 100, 120 and 140 kSeeds ha^{-1}), calculated according to the SFI measured with an on-line vis-NIRS sensor.

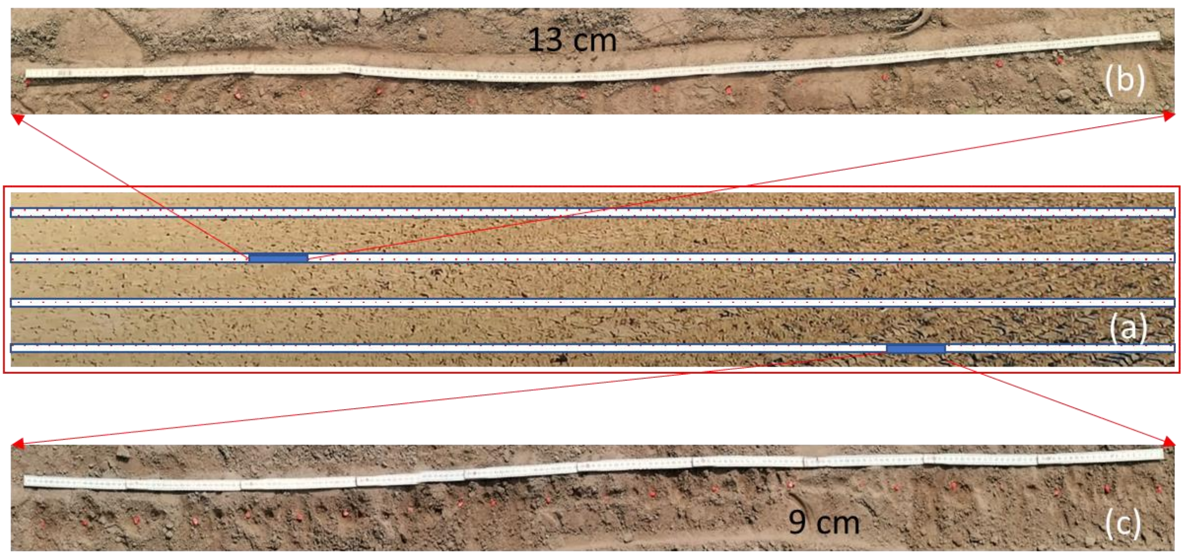

Figure 4 Schematic diagram of the (a) calibration test plot seeded with the proposed sensor-based site-specific seeding system. (b) and (c) shows two examples of in-row sections where seed rates were counted and recorded.

2.5 In-field implementation

A 5 ha field located at Melle region (50∘59′10.5′′N 3∘49′04.1′′E) in Belgium was selected. It resides under the temperate maritime climate with an annual average temperature ranging between 6 to 10 °C and precipitation varies from 700 to 850 mm (Peeters, 2010). The field has flat terrain with a mild undulation of altitude of up to 2.5 m. Soil texture analysed with the sieve and pipette method is a silt-loam with a clay content ranging from 5.7 to 16.1%, and sand content from 9.2 to 42.6%. A typical crop rotation of potato/sugar beets, wheat/maize with a seasonal cover crop is followed. Maize was also grown in the previous season of that of the current study, which breaks the regular crop rotation by growing maize after maize.

The field was ploughed with a disc plough to primarily open the soil. Secondary tillage was carried out by rotavator, spike and drum harrows to prepare seedbed on the day before maize sowing on the 16th of June 2021. The seeding machine (Kverneland Optima Rigid e-Drive, The Netherlands) was connected to the tractor (New Holland T5.110, USA; engine power = 79 kW) CANbus through the ISObus cable, and an in-cab connector was used to connect the Tellus PRO to communicate with the seeding machine. A laptop installed with the proposed software was connected with Tellus PRO. After calibrating the vis-NIRS sensor, field sowing kicked off (Figure 1 b). Maize hybrid of SY Talisman was selected in this study since it is a cultivar of dual-use for grain and silage production, and is known for its very strong early vigour, very high and stable yielding characteristics under stress conditions, tolerance to the heat up and suitability for all types of soil. Planter depth was set at 2.5 cm and the tractor was driven at a speed of 5 km hr^{-1}. After completion of field sowing, soil spectral data, on-line predicted SFI, calculated and applied seed rate were exported for further analysis.

2.6 Crop management and harvesting

The field was fertilized with 100 kg N ha^{-1} and 220 kg K ha^{-1} at the time of soil preparation, and 120 kg P ha^{-1} was side-dressed at the time of field sowing. A second round of 50 kg N ha^{-1} was sprayed 45 days after planting. Herbicides were sprayed at the 3–4 leaf stage to control the weed infestations. The crop was grown under a rainfed production system.

There were several repeated checks of the crop canopy to see whether the dry matter reached the desirable range between 30 to 38% of above ground plant biomass. The whole plant's dry matter was investigated by looking at the milk line of the grain (DuPont, 2013). Finally, on 17th November 2021, the crop was harvested as silage maize using a combine harvester equipped with a yield monitoring system (John Deere, model-9700, Moline, IL, USA). The silage yield was estimated by measuring crop mass-flows (throughput) per second with an average travel speed of 6 km hr^{-1} while location is recorded by a global navigation satellite system.

2.7 Silage yield and economic analysis

Yield data from the combine harvester was firstly cleaned by removing the unexpected records e.g., NAs, zeros etc. Also, the yield samples located at the field buffer region (19 m each at the three of four sides of the field) were discarded from the analysis (Figure 5). Yield observations were superimposed over the applied seed rate map. In order to compare the yield and economic return of SSS against the URS, a total of ten sub-plots of URS treatment were identified in locations where the recommended seed rate of 90 kSeeds ha^{-1} was planted. This means that the width of these ten sub-plots should at least cover two parallel passages of the seeding machine, over which at least one passage of the combine harvester is encountered. This was necessary to avoid any possible overlapping in the yield observations from different seeding rates since the combine harvester used in this study cut 8 rows at a time whereas the planter sowed four rows. Yield observations located within these ten subplots were extracted and analysed as the yield of the URS treatment, whereas the yield observations for the remaining parts of the field were considered as the yield of SSS treatment. An average yield of each seeding treatment was used for the cost-benefit analysis, using the partial budgeting approach (Roth, 2017) in map-based SSS. Partial budgeting focuses only on the changes in income and expenses that would result from implementing a specific alternative. Thus, all aspects of farm profits that are unchanged by the decision can be safely ignored. The revenue, silage yield (t ha^{-1}) multiplied by the market price of 60 € t^{-1}, was considered as the production outcome while the seed costs (180 € ha^{-1}; when seed rate is 100 kSeeds ha^{-1}) were assumed as the input cost of production. Note that all other costs such as land preparation, fertilizer, herbicide, pesticides, and harvesting costs were assumed to be constant for both URS and SSS treatments.

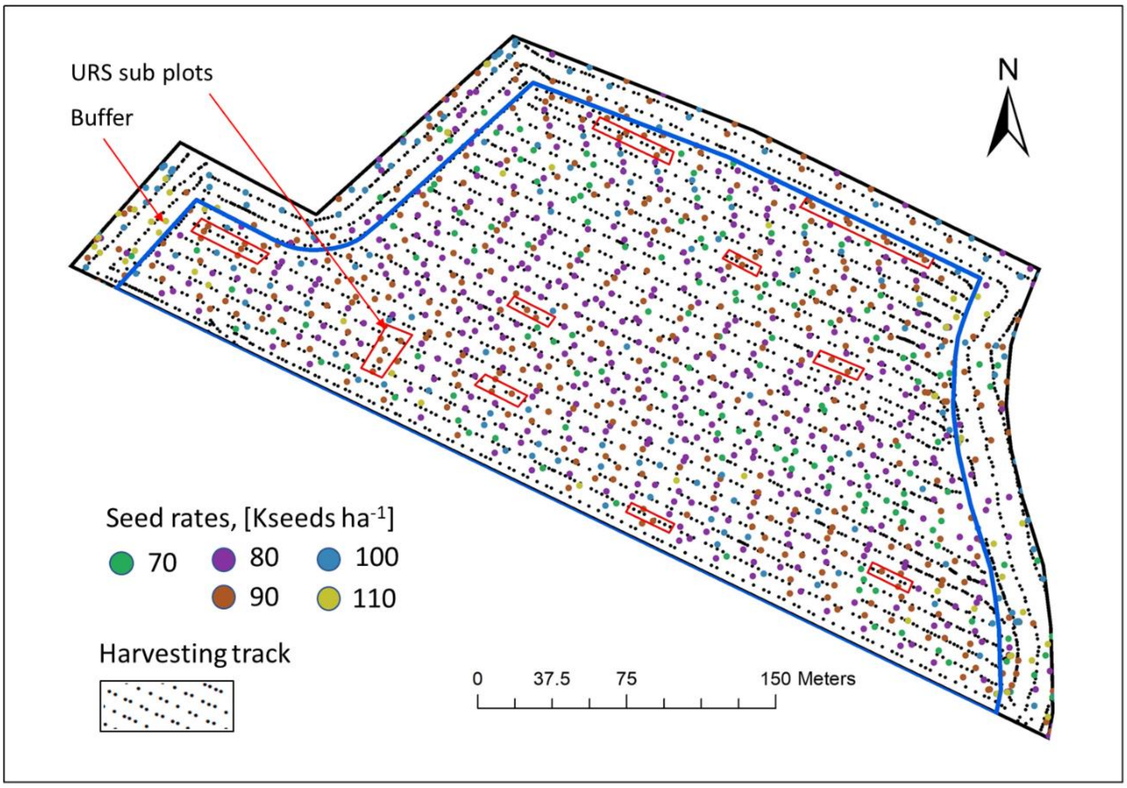

Figure 5 Point features map of applied seed rates, silage harvesting tracks, and uniform rate seeding (URS) sub-plots (within rectangular).

2.8 Mapping

On-line predicted SFI, applied seed rate, and yield records were of georeferenced points data. To explore the spatial pattern and distribution of those parameters, spatial interpolation was followed to create surface data from these sample points. Individual variogram model was developed for each parameter before ordinary kriging interpolation using the function available in "geostatistical analyst" tools in ArcGIS (ESRI ArcGIS™ version 10.7.1, CA, USA).

2.9 Statistical analysis

The accuracy of controlling the seed rate by the proposed system was calculated using the following equation.

$$\eta = \left(1 - \frac{|S_d - S_a|}{S_d}\right) \times 100$$

Where, η = seed rate control efficiency; S_d and S_a = defined and actual seed rate, respectively. For the exploration of applied seed rates, on-line predicted SFI and observed yield, the descriptive statistics were calculated. To understand the strength of association between the predicted SFI and actual seed rates, a linear regression model was fit. The goodness of fit was evaluated using the coefficient of determination (R^2) and root mean square error (RMSE). The t-test statistics were used to investigate whether regression coefficients were statistically significant at a 95% confidence interval. In addition to the yield data exploration, Welch's two-samples t-test statistics were determined to check if the mean yield of URS and SSS treatments were different at a 95% level of significance.

3 Results and discussion

3.1 System accuracy

The calibration results showed that the proposed sensor-based SSS system was 87.5% accurate for maintaining the defined seed rate while its accuracy varied from 77.8 to 95.2% (Figure 6).

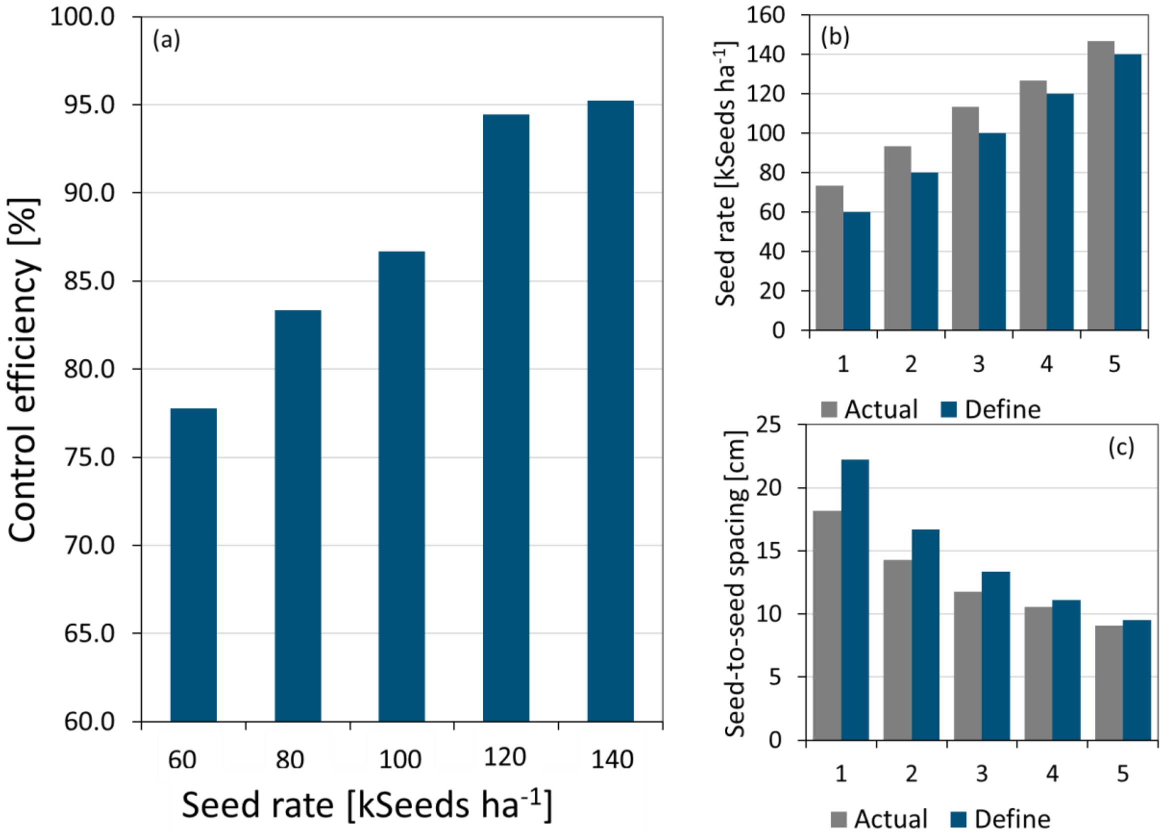

Figure 6 Accuracy of sensor-based site-specific seeding system in controlling calculated seed rate (a), and deviation between calculated vs actual seed rate (b) and seed-to-seed spacing (c) observed for the calibration test. 1, 2, 3, 4 and 5 stand for the number of observations.

The lowest accuracy was observed for the lowest seed rate of 60 kSeeds ha^{-1}, and accuracy was increased successively to reach 95.2% for the highest seed rate of 140 kSeeds ha^{-1}. The maximum deviation between the actual and defined seed-to-seed (StS) spacing was 4 cm for the lowest seed rate, which was reduced to 0.4 cm for the highest seed rate. This means that the proposed system was less accurate to control the desired seed rate and thus StS spacing for seed rates lower than 120 kSeeds ha^{-1}. It is important to note that, the proposed seeding system always sowed a higher seed rate than the target seed rate by 6.7 to 13.7 kSeeds ha^{-1}. This could be explained by the slow planter driving speed of 3.5 km hr^{-1} than the manufacturer recommended speed of 5 to 7 km hr^{-1} for smooth actuation of various seeding rates, which might result in sowing seeds at different locations from those of the sensing points. However, a driving speed of 5.0 km hr^{-1} was selected in the actual field implementation to match the manufacturer's recommended speed and to avoid any lapse time between soil sensing and seed actuating. One more reason could be the large range of seed rates (60 to 140 kSeeds ha^{-1}) considered during the calibration test, which led to the planter facing big jumps while switching between successive seed rates. As a measure of minimizing the seed rate switching error, a relatively lower range (70 to 110 kSeeds ha^{-1}) of seed rates was adopted during the actual field application so that the planter switches different seed rates smoothly.

3.2 Soil fertility status and seed rate statistics

Summary statistics of soil SFI and applied seed rates are shown in Figure 7. The SFI results indicate that the current field had a moderate fertility status (average SFI = 4.8) and variation (interquartile range of SFI = 2.3) with a normal distribution pattern. Despite the fact that the on-line vis-NIRS sensor measured SFI of this field at a high sampling resolution of 6770 scanning points, this was reduced after averaging 5 scans into one. This is the reason why SFI and seed rate observations were shown for a lower resolution of 1354 observations per field. Seed rate statistics (Figure 7 b) indicated that the major area of the field was sown with a seed rate of 80 kSeeds ha^{-1}. The second large area of the field was seeded with 90 kSeeds ha^{-1} and successively followed in descending order by 100, 70, and 110 kSeeds ha^{-1}, indicating that only a small area of the field had high SFI values ($8 \leq$ SFI ≤ 10). As a result, the proposed system recommended an average seed rate of 86.4 kSeeds ha^{-1}, which is lower than the seed rate used for URS system (90 kSeeds ha^{-1}), thanks to the advanced on-line vis-NIRS sensing system, which enabled successful assessment of SFI in real-time, for calculation of seed rates to match the in-field heterogeneity in soil fertility.

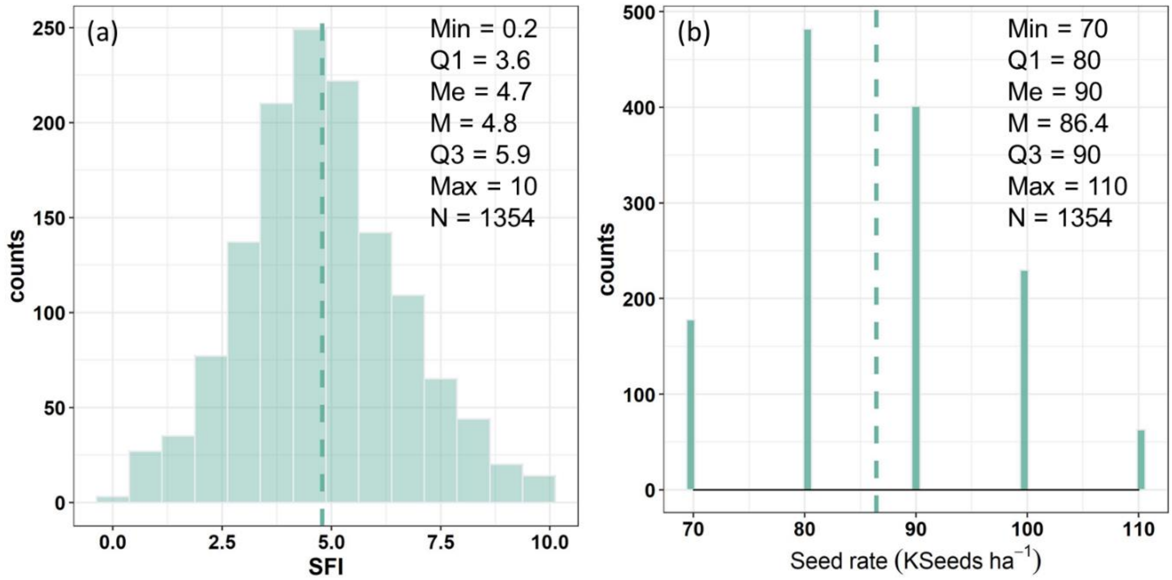

Figure 7 Summary statistics of (a) soil fertility index (SFI) and (b) applied seed rates. The dotted lines indicate the mean values. Min, minimum; Me, median; M, mean; Q1 and Q3, 1st and 3rd quartile; Max, maximum; N, number of observations.

3.3 Association between soil fertility and seed rates

Maps of seed-rate applied and on-line predicted SFI were very similar (Figure 8). As can be observed that the major part of this field has low fertility (SFI < 4.9) that is now the middle part of the field. A wide strip along the bottom edge has moderate-to-high fertility (SFI = 5 to 6), except a part near the bottom right corner (circle-iii in Figure 8). The highest fertility values were observed at the top-right corner and left edge (north-west) of the field. Field observations show that the top-right corner soil (circle-ii) is of a relatively heavier soil and lower in elevation than the rest of the field. The highest fertility at the left edge could be attributed to the nutrients transported from the cattle waste since an animal farm is located next to this edge of the field. All these key features in SFI spatial variability showing strong similarity with seed rate map (Figure 8), prove that the proposed sensing, modelling and controlling system led to accurate placement of seed rates according to the spatial variability in soil fertility indicated as SFI.

When seed rate values had been regressed against corresponding SFI values at the same position, a strong linear relationship was established with an R^2 of 0.80 (Figure 8), and RMSE of 5.4 kSeeds ha^{-1}, and the regression was found statistically significant ($p < 2.2e-16$). Its intercept of 61.2 kSeeds ha^{-1} indicates that zones in the field with the least fertility index can support a maximum seed rate of 61.2 kSeeds ha^{-1}. Beyond this minimum value, each unit increase in SFI supports an increase in the seed rate of 5.3 kSeeds ha^{-1}. The remaining 20% inaccuracy of regression could be due to the wrong seed rate assignments and error in recording the actual seed rate sown in the field. The time-lapse between sending and receiving seed rate messages to and from the VR controller could be the most critical reason. Other reasons could be the machine vibration, soil clods and the error of the on-line assessment of SFI with vis-NIRS sensor [$R^2 = 0.75$ (Munnaf & Mouazen, 2021)]. It is, therefore, suggested that further study is needed to understand better the operational conditions of the system to enable more robust and accurate SSS field application. Furthermore, a science-based relationship between SFI and recommended seed rate should be established to ensure the correct rate applied according to the soil fertility level. However, extensive field trials need to be carried out and repeated for several cropping seasons to collect enough agronomic data to establish a mathematical relationship that insures the highest yield for different values of SFI. Since this work intends to prove a concept of an advanced technological solution on the vis-NIR sensor-based SSS, the focus was on the technological development rather than on the creation of optimal seeding recommendations that guarantee the best yield and economic benefits, with the latter to be discussed in the following section.

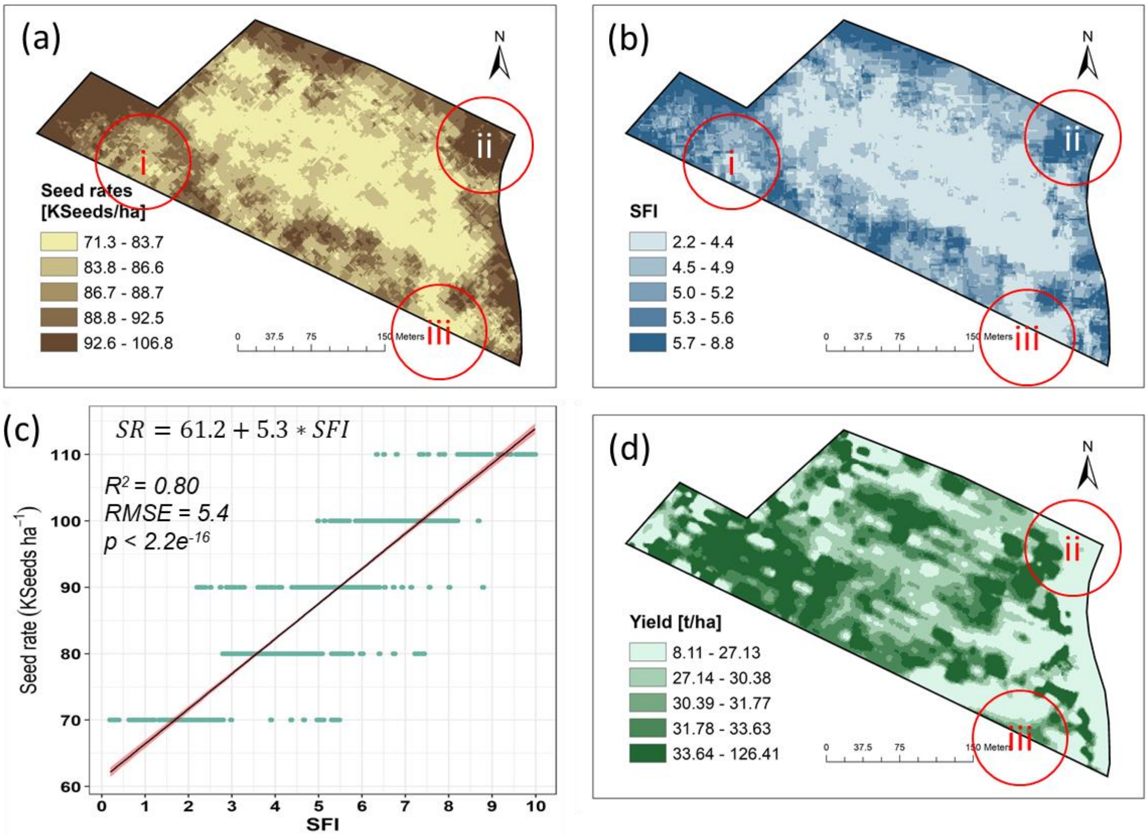

Figure 8 Maps of (a) applied seed rates (SR), (b) on-line soil fertility index (SFI) and (c) linear relationship between SFI and SR, and (d) silage maize yield. Red shadow around the regression line indicates 95% confidence interval. Circles with the same number highlight similarity in the respective variations.

3.4 Productivity and profitability analysis

Table 1 shows the summary statistics of silage yield observed under both URS and SSS treatments. The proposed SSS produced a mean silage yield of 33.0 t ha^{-1} while the URS produced a slightly lower silage yield of 31.6 t ha^{-1}. This yield improvement by SSS was not statistically significant at 95% (p=0.18) according to a two-sample t-test (Figure 9). Larger variations were calculated for SSS (CV = 35.3%) than URS (CV = 29.3%). The higher CV value of SSS can be explained by its yield increases that increases dispersion of readings around the mean. However, SSS has led to an almost homogenous yield range across the largest areas of the field when compared with the SFI (CV = 37.3%) map of field (Figure 8).

Table 1 Maize silage yield statistics calculated for the uniform rate seeding (URS) and site-specific seeding (SSS) treatments.

Seeding treatment	Silage yield statistics								
	Min	Q1	Median	Mean	Q3	Max	SD	CV, %	n
URS	14.1	24.7	30.3	31.6	36.2	53.7	9.25	29.3	85
SSS	9.56	27.6	31.9	33.0	35.7	145.0	11.6	35.3	2089

Q1 and Q3, first and third quartile, respectively; SD, standard deviation; CV, coefficient of variance; n, number of observations.

Most importantly, the middle part of the field having the lowest SFIs provided a similar yield as that of the high fertility zones e.g., the major part of the long strip along the bottom edge of the field. A similar yield improvement cannot be observed in the remaining part of this strip at the right end (circle iii in Figure 8), which may well be explained by the high moisture content (MC) of this part (Figure 10 a), having a heavier soil texture, being lower in altitude (Figure 10 b), and perhaps having poor drainage. These field characteristics resulted in high fertile zone and thus sown with high seed rates (circle ii in Figure 8), though could not yield optimally. Despite the MC map being measured in 2018 (not used for SFI prediction in 2021) using the same sensor (Figure 10 a), the spatial distribution pattern does not change, although the magnitude changes. Indeed, MC was the most important crop growth-limiting factor in the 2021 cropping season, as precipitation was very intensive and in some places caused flooding events not encountered in the last 100 years. Moreover, the Eastern edge of the field suffered from the shadow of big trees along this edge, limiting crop growth and yield despite the high SFI measured. A drastic reduction in germination was observed in this part of the field.

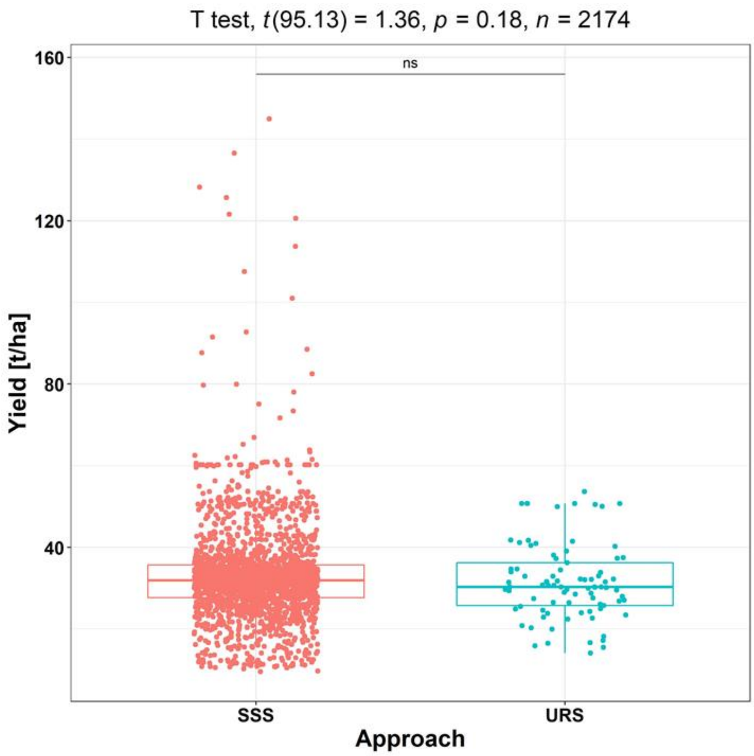

Figure 9 Jitterbox plot together with the Welch two-samples t-test statistics calculated for maize silage yield in uniform rate seeding (URS) and site-specific seeding (SSS) treatments. ns stands for non-significant pair at 95% confidence.

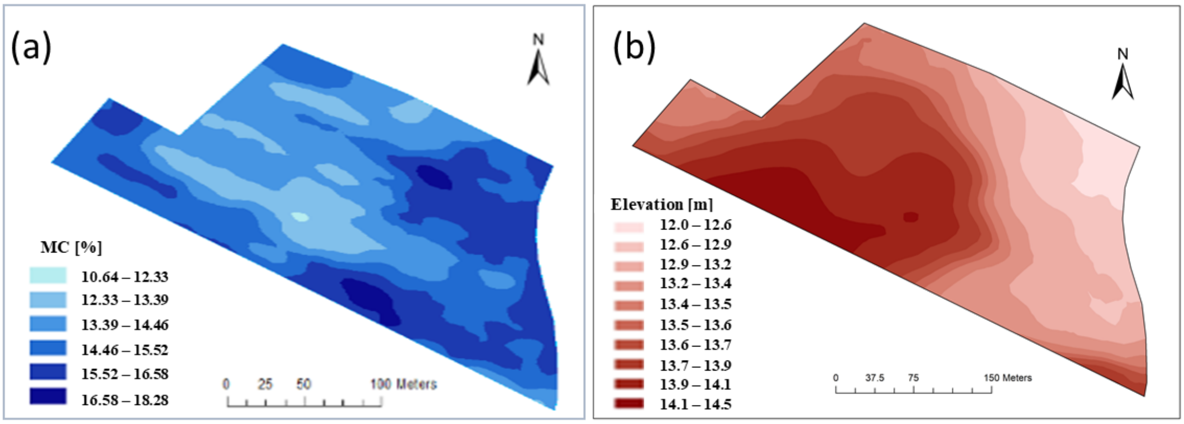

Figure 10 Maps of (a) soil moisture content (MC) predicted with the on-line visible and near infrared spectroscopy (vis-NIRS) sensor in 2018, and (b) elevation map obtained from the yield monitoring system of the combine harvester.

Table 2 Cost-benefit analysis of site-specific seeding (SSS) on silage maize, compared to the uniform rate seeding (URS).

Accounting items	Seeding treatments	
	URS	SSS
Average seed rate, kSeeds ha^{-1}	90	86.4
Seeding cost, € ha^{-1}	162	156
Yield, t ha^{-1}	31.6	33.0
Revenue, € ha^{-1}	1896	1980
Gross margin, € ha^{-1}	1734	1825
Relative gross margin[a], € ha^{-1}	-	91
Return on yield[a], € ha^{-1}	-	84
Seed cost saving[a], € ha^{-1}	-	7
Gross margin variation[a], %	-	5.2

[a]Values were calculated in comparison with URS; kSeeds, 1000 seeds; Assumptions: maize seed cost = 180 € ha^{-1} at a seed rate of 100 kSeeds ha^{-1}, silage market price = 60 € t^{-1}.

Similar to the yield improving trend, the proposed sensor-based SSS improved gross margin in comparison with the URS by means of increasing silage yield as well as saving on the seed costs (Table 2). The URS treatment produced a field gross margin of 1734 € ha^{-1}, while the SSS increased the gross margin to 1825 € ha^{-1}, providing an extra relative gross margin of 91 € ha^{-1}, of which only 7 € ha^{-1} was due to saving on the reduced amount of seeds applied. Overall, the SSS increased gross margin by 5.2%, compared to the URS. These findings are in line with those by (Munnaf et al., 2022), who reported an improved gross margin of 92.67 € ha^{-1} for map-based SSS of grain maize and a much larger gross margin for map-based SSS in potato (Munnaf et al., 2020; Munnaf et al., 2021; Munnaf & Mouazen, 2021). The SSS was not frequently reported to save from seeding costs, unlike this study. Munnaf et al. (2022) reported that the map-based SSS of grain maize consumed slightly higher seed rates than the URS, and this dropped the gross margin by 4.65–7.36 € ha^{-1} in most cases. However, a saving in seed costs of 4.64 € ha^{-1} was observed for one treatment of a map-based SSS of grain maize at this same study site in 2020. A much lower maximum net return to seed cost of 2.2 € ha^{-1} was observed with a seed rate of 76.3 kSeeds ha^{-1} (Coulter et al., 2010). Several studies also showed that the production margin of SSS is attributed to the yield increase than saving on input seeding costs (Dwight et al., 2013; Lovell, 2016; Munnaf et al., 2020; Munnaf et al., 2021). Since no other sensor-based SSS studies for silage maize exist, no comparative figures could be provided to show how good the gross margin was compared to previous work. However, technically speaking, the current study proved for the first time that sensor-based SSS for silage maize is possible and that it is economically viable. Therefore, the proposed system can be seen more as a technological development than economic achievement, however, the cost-benefit analysis provides the first impression of its economic feasibility that is likely to motivate farmers.

4 Conclusions

A fully automated sensor-based site-specific seeding technology was developed and implemented, whose agronomic and economic potentials were evaluated for silage maize production in one field. The system consists of an on-line vis-NIRS sensor to measure SFI, a decision support system to calculate seed rates according to the measured SFI and a seeding machine for applying the recommended seed rate. The on-line vis-NIRS sensor predicted SFI accurately and mapped considerable spatial variation in soil fertility, which necessitates SSS. The proposed system may well be expected to be 87.5% accurate in controlling the desired seed rates according to the measured SFI at a slow driving speed. The predicted SFI and applied seed rates showed a strong linear relationship (R^2 = 0.80) as well as similar spatial distribution patterns over the field. As a result, this SSS improved silage yield by 1.4 t ha^{-1} (4.4%), while sowing a lower seed rate (86.4 kSeeds ha^{-1}) than the URS (90 kSeeds ha^{-1}). This has resulted in an improvement of gross margin by 91 € ha^{-1}, of which only 7 € ha^{-1} was attributed to savings on seed cost. The yield increased by the SSS was not statistically significant. However, the proposed fully automated sensor-based SSS can be considered as a prospective tool for improving production margin by managing soil heterogeneity. The proposed sensor-based SSS system has become a reference from technological point of view, and opened a window for further development in future. Future works are suggested to evaluate the agronomic and economic benefits of the proposed system under larger number of fields to prove the observed benefits in the current work. Since this study was limited to a single field silage maize case study, further studies are encouraged for grain maize in different soil types, weather conditions under different agricultural systems over several cropping seasons. Future studies should establish mathematical relationships to calculate the seed rate as a function of SFI based on agronomic data collected from field trials.

Acknowledgment

Authors acknowledge the financial support received from the Research Foundation - Flanders (FWO) for Odysseus I SiTeMan Project (Nr. G0F9216 N).

References

Andrews, S.S., Karlen, D.L., Cambardella, C.A., 2004. The Soil Management Assessment Framework. Soil Sci. Soc. Am. J. 68, 1945. https://doi.org/10.2136/sssaj2004.1945

Chattha, H.S., Zaman, Q.U., Chang, Y.K., Read, S., Schumann, A.W., Brewster, G.R., Farooque, A.A., 2014. Variable rate spreader for real-time spot-application of granular fertilizer in wild blueberry. Comput. Electron. Agric. 100, 70–78. https://doi.org/10.1016/j.compag.2013.10.012

Coulter, J.A., Nafziger, E.D., Janssen, M.R., Pedersen, P., 2010. Response of Bt and near-isoline corn hybrids to plant density. Agron. J. 102, 103–111. https://doi.org/10.2134/agronj2009.0217

DuPont, 2013. Maize Silage Harvest Management, Maturity & Ensiling [WWW Document]. DuPont Pioneer. URL https://www.pioneer.co.nz/inoculants/product-information/the-complete-guide-to-harvesting-maize-silage/harvest-management/ (accessed 1.15.22).

Dwight, K., Craig, K., Grant, H., Farrell, A., 2013. Variable Rate Seeding: Easier Than You Think - Crop Quest Agronomic Services [WWW Document]. CropQuest. URL https://www.cropquest.com/variable-rate-seeding/ (accessed 5.7.18).

Esau, T.J., Zaman, Q.U., Chang, Y.K., Groulx, D., Schumann, A.W., Farooque, A.A., 2014a. Prototype variable rate sprayer for spot-application of agrochemicals in wild blueberry. Appl. Eng. Agric. 30, 717–725. https://doi.org/10.13031/aea.30.10613

Esau, T.J., Zaman, Q.U., Chang, Y.K., Schumann, A.W., Percival, D.C., Farooque, A.A., 2014b. Spot-application of fungicide for wild blueberry using an automated prototype variable rate sprayer. Precis. Agric. 15, 147–161. https://doi.org/10.1007/s11119-013-9319-4

Grisso, R., Alley, M., Thomason, W., Holshouser, D., Roverson, G.T., 2011. Precision Farming Tools: Variable-Rate Application. Virginia Coop. Ext. 1–7.

Guerrero, A., De Neve, S., Mouazen, A.M., 2021. Current sensor technologies for in situ and on-line measurement of soil nitrogen for variable rate fertilization: A review, in: Advances in Agronomy. Academic Press, pp. 1–38. https://doi.org/10.1016/bs.agron.2021.02.001

Isbell, N., 2005. Variable-Rate Seeding. Alabama Precis. Ag Ext. 1–3.

Jiang, W., Wang, K., Wu, Q., Dong, S., Liu, P., Zhang, J., 2013. Effects of narrow plant spacing on root distribution and physiological nitrogen use efficiency in summer maize. Crop J. 1, 77–83. https://doi.org/10.1016/j.cj.2013.07.011

Kempenaar, C., Been, T., Booij, J., van Evert, F., Michielsen, J.M., Kocks, C., 2017. Advances in Variable Rate Technology Application in Potato in The Netherlands. Potato Res. 60, 295–305. https://doi.org/10.1007/s11540-018-9357-4

Lovell, A., 2016. Variable-rate seeding next step in precision farming [WWW Document]. Seeding Tillage Focus Southwest corn Grow. reports High. yield Low. seed costs, Manitoba Co-operator. URL https://www.manitobacooperator.ca/crops/variable-rate-seeding-next-step-in-precision-farming/ (accessed 5.7.18).

Maleki, M.R., Mouazen, A.M., De Ketelaere, B., Ramon, H., De Baerdemaeker, J., 2008. On-the-go variable-rate phosphorus fertilisation based on a visible and near-infrared soil sensor. Biosyst. Eng. 99, 35–46. https://doi.org/doi:10.1016/j.biosystemseng.2007.09.007

Maleki, M.R., Zamiran, A., 2009. Evaluating the profitability of a soil sensor-based variable rate applicator for on-the-go phosphorus fertilization. Int. J. Agric. Biol. 11, 651–658.

Mouazen, A.M., 2006. Soil Survey Device. International publication published under the patent cooperation treaty (PCT). World Intellectual Property Organization, International

Bureau. International Publication Number: WO2006/015463; PCT/BE2005/000129; IPC: G01N21/00; G01N21/00

Mouazen, A.M., Kuang, B., 2016. On-line visible and near infrared spectroscopy for in-field phosphorous management. Soil Tillage Res. 155, 471–477. https://doi.org/10.1016/j.still.2015.04.003

Munnaf, M.A., Haesaert, G., Mouazen, A.M., 2022. Site-Specific Seeding for Maize Production Using Management Zone Maps Delineated with Multi-sensors Data Fusion Scheme. Soil Tillage Res. 220, [in revision]. https://doi.org/10.1016/j.still.2022.105377

Munnaf, M. A., Haesaert, G., Mouazen, A.M., 2020. Map-based site-specific seeding of seed potato production by fusion of proximal and remote sensing data. Soil Tillage Res. 206, 104801. https://doi.org/10.1016/j.still.2020.104801

Munnaf, M.A., Haesaert, G., Van Meirvenne, M., Mouazen, A.M., 2021. Multi-sensors data fusion approach for site-specific seeding of consumption and seed potato production. Precis. Agric. https://doi.org/10.1007/s11119-021-09817-8

Munnaf, M.A., Haesaert, G., Van Meirvenne, M., Mouazen, A.M., 2020. Map-based site-specific seeding of consumption potato production using high-resolution soil and crop data fusion. Comput. Electron. Agric. 178, 105752. https://doi.org/10.1016/j.compag.2020.105752

Munnaf, Muhammad Abdul, Mouazen, A.M., 2021a. Optimising site-specific potato seeding rates for maximum yield and profitability. Biosyst. Eng. 212, 126–140. https://doi.org/10.1016/j.biosystemseng.2021.10.006

Munnaf, Muhammad Abdul, Mouazen, A.M., 2021b. Development of a soil fertility index using on-line Vis-NIR spectroscopy. Comput. Electron. Agric. 188, 106341. https://doi.org/10.1016/j.compag.2021.106341

Munnaf, Muhammad A., Mouazen, A.M., 2021. Optimising site-specific potato seeding rates for maximum yield and profitability. Biosyst. Eng. 212, 126–140. https://doi.org/10.1016/J.BIOSYSTEMSENG.2021.10.006

Peeters, A., 2010. Country pasture/forage resource profile for Belgium [WWW Document]. FAO. URL http://www.fao.org/ag/AGP/AGPC/doc/Counprof/Belgium/belgium.htm.

Roth, S., 2017. Partial Budgeting for Agricultural Business. Publ. Distrib. Center, Pennsylvania State Univ., Fourth 1–8.